Online-Journals.org

iJOE International Journal of Online and Biomedical Engineering

iJOE | eISSN: 2626-8493 | Vol. 21 No. 3 (2025) | OPEN ACCESS

https://doi.org/10.3991/ijoe.v21i03.53231

PAPER

Development of Linear Contrast Stretching (LCS) and Region of Interest (ROI) Method for Detecting Spinal Fractures Based on CT-Scan Images

Sri Rahmawati[1](✉), Iskandar Fitri[2], Gunadi Widi Nurcahyo[2]

[1]Information System, Faculty of Computer Science, Universitas Putra Indonesia YPTK, Padang, Indonesia

[2]Information Technology, Faculty of Computer Science, Universitas Putra Indonesia YPTK, Padang, Indonesia

sri_rahmawati@upiyptk.ac.id

ABSTRACT

This study aims to develop linear contrast stretching (LCS) and region of interest (ROI) methods to detect spinal fractures based on CT-scan images. LCS is applied to enhance image contrast by expanding the pixel intensity range, thereby clarifying bone structure. ROI is used to focus the analysis on relevant areas, such as sections of bone suspected to have fractures. The development of these LCS and ROI methods is expected to improve fracture detection visibility, as evidenced by more precise measurement of the detected fracture pixel area and increased detection accuracy, which is anticipated to facilitate the clinical diagnosis process. The study consists of several stages, including image preprocessing, edge detection, image sharpening, and the application of LCS + ROI on the targeted area. The study findings indicate that the proposed method is capable of detecting fractures with high accuracy, thereby assisting radiologists in diagnosing spinal fractures more quickly and accurately, achieving an accuracy rate of 95%. The implementation of this method is expected to make a significant contribution to CT-scan image-based medical diagnosis.

KEYWORDS

linear contrast stretching (LCS), region of interest (ROI), spinal fractures, vertebrate fracture sufferers, CT-scan images

1 INTRODUCTION

A spinal fracture is a complete or partial break in the spine or vertebral bones [1]. It is a serious medical condition that can significantly impact a person's mobility and overall quality of life [2]. The most common causes of spinal fractures include trauma from falls, traffic accidents, sports injuries, and physical violence [3], [4]. Additionally, osteoporosis and other bone-weakening conditions can cause fractures even from minor injuries [5]. Common diagnostic tools include routine

Rahmawati, S., Fitri, I., Nurcahyo, G.W. (2025). Development of Linear Contrast Stretching (LCS) and Region of Interest (ROI) Method for Detecting Spinal Fractures Based on CT-Scan Images. *International Journal of Online and Biomedical Engineering (iJOE)*, 21(3), pp. 165–182. https://doi.org/10.3991/ijoe.v21i03.53231

Article submitted 2024-11-08. Revision uploaded 2024-12-26. Final acceptance 2024-12-26.

© 2025 by the authors of this article. Published under CC-BY.

X-rays [6], [7], CT scans [8], [9], and MRI [10], [11] to assess the extent of fractures and any associated soft tissue damage. Linear contrast stretching (LCS) is an image processing technique designed to enhance image contrast by expanding the pixel intensity range to cover the entire available intensity range, for example, from 0 to 255 in eight-bit images [12]. LCS works by identifying the minimum and maximum intensity values in the original image, then using a linear transformation to spread the pixel intensity values across the new range [13]. On the other hand, the region of interest (ROI) is a specific part of an image selected for further analysis or processing, usually because that area contains critical information for study or examination [14], [15]. The implementation of LCS in digital image processing, particularly in CT-scan images, enhances the visibility of medical structures such as bones or soft tissues that may not be clearly visible in the original image. By applying LCS, doctors can more easily detect abnormalities like spinal fractures. ROI is used to focus the analysis on specific relevant areas, such as regions suspected of having fractures [16]. Using LCS within an ROI can clarify essential features in that area, supporting a more accurate and efficient diagnosis [17]. Therefore, the combination of LCS and ROI in CT-scan image processing improves visual quality and medical detection effectiveness, aiding healthcare professionals in making better clinical decisions [18].

This study was previously conducted by Ruikar et al. [19]. These researchers performed automated segmentation and labeling of fractured bones from CT-scan images. The goal of the study was to develop an automated method for segmenting and labeling fractured bones in CT images. The method involved using LCS to enhance image contrast, making it easier to identify fractured bones. The results showed that this technique successfully improved the visibility of bone details by up to 85%, reduced unwanted artifacts, and enabled highly accurate labeling of fractured bones. The study concluded that LCS is an effective technique for enhancing CT image quality and supports better diagnosis and surgical planning. A similar study was conducted by Jeong et al. [20] assessed the diagnostic performance of dual-energy CT-scan in detecting acute spinal fractures. This study aimed to evaluate the diagnostic performance of dual-energy CT for detecting acute spinal fractures. The study utilized LCS to enhance contrast and detail in spinal fractures on CT images. The findings demonstrated an increase in spinal fracture detection accuracy by 92%, with improved visibility and a reduction in diagnostic errors. The study concluded that LCS significantly enhances the accuracy of diagnosing acute spinal fractures.

To enhance the clarity of this study, the research question has been explicitly defined as: How can LCS and ROI methods be optimized to improve the accuracy and efficiency of spinal fracture detection in CT-scan images? This question guides the development of methodologies aimed at addressing limitations in current fracture detection approaches. Furthermore, the literature review has been expanded to include recent studies on advanced imaging techniques, such as convolutional neural networks (CNN) in medical diagnostics and dual-energy CT-scan applications. These studies demonstrate significant improvements in fracture detection, emphasizing the relevance and timeliness of the proposed method.

This study builds upon recent advancements in the field of spinal fracture detection, incorporating state-of-the-art findings to ensure a comprehensive approach. Notable references include research on automated fracture detection using artificial intelligence, dual-energy CT-scan technology, and improvements in image processing algorithms for enhanced medical imaging. These additions reflect

the rapid developments in the field and provide a solid foundation for the proposed methods. By integrating these references, this manuscript offers a holistic perspective, bridging traditional techniques with modern innovations in medical imaging. The proposed methodology integrates LCS and ROI methods into a novel regional contrast stretching (RCS) algorithm specifically tailored for spinal fracture detection using CT-scan images. This approach goes beyond standard image analysis by focusing on optimizing contrast within the ROI to improve detection accuracy. The novelty lies in the algorithm's ability to enhance localized features, facilitating more precise identification of fracture patterns compared to existing methods. This contribution positions the study as a step forward in medical imaging innovation, particularly in addressing limitations of conventional diagnostic tools. This study aims to develop LCS and ROI methods in spinal CT-scan images to detect cracks or fractures in the spine more accurately. This development builds upon previous research findings, especially the ideas of Ruikar et al., Jeong et al., and Hanson et al., who succeeded in improving image quality and fracture detection accuracy. The goal of this study is to detect spinal cracks based on spinal CT-scan images by developing the LCS and ROI methods.

2 MATERIALS AND METHODS

2.1 Research framework

The research framework was designed and implemented systematically to ensure that the outcomes remain aligned with the objectives set at the beginning of the study as the researcher proceeds. This study's research framework outlines the steps taken to resolve the issue being discussed. Figure 1 shows the research framework of this study.

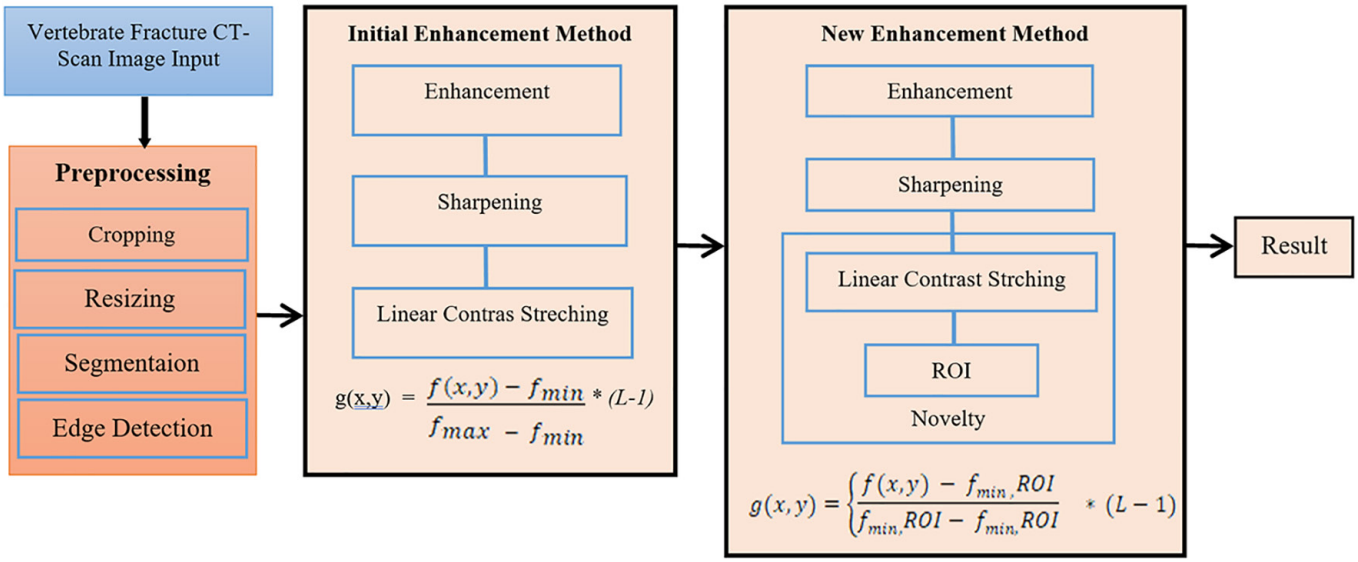

Fig. 1. Research framework

Figure 1 illustrates the research framework applied to identify vertebral fractures in spinal CT-scan images and to understand the diagnostic results from

image analysis. The first stage involves collecting the original images to be used as test images for the study. The images used in this test are sagittal CT-scan images of the spine from M. Djamil central general hospital (RSUP) in Padang. Images were obtained using CT-scan equipment, with each patient having multiple image slices. The second stage is the preprocessing phase, which includes processes such as cropping (to trim the image), resizing (to adjust the image dimensions), segmentation, and edge detection. The third stage involves the initial enhancement process to improve the quality of the spinal images so that they are clearer and the information within them can be accurately extracted. Images that are too bright or too dark can obscure the information they contain. This stage is followed by image sharpening to clarify image details and enhance the quality of images that may have become blurred, either due to errors or as a result of specific image acquisition methods. LCS is applied to increase contrast, especially in images with low contrast. The fourth stage involves results detection by combining the LCS algorithm and the ROI method to create a new algorithm called RCS. This algorithm is used to determine the outcome of CT-scan images showing anomalies (fractures), allowing for a clear diagnosis of patients with spinal issues.

2.2 Input of CT-scan spine test image

This section represents the initial stage, involving the collection of CT-scan image data of the spine to be tested in this study. The original images used as input data are sagittal spine CT-scan images in *.jpg format, sourced from CT scans at M. Djamil Hospital, Padang, without discussing the image acquisition process. Figure 2a highlights the structure of a normal spine, while Figure 2b shows distinct fracture lines in the vertebrae.

Fig. 2. Sagittal image of the spine: a) Normal, b) Fracture

The dataset for this study comprises sagittal CT-scan images of 83 patients collected from M. Djamil Central General Hospital, Padang. The images include both normal and fractured spine cases, ensuring diversity and representativeness. The patient demographics range from adults to elderly individuals, covering varying degrees of fracture severity. Images were acquired using a standardized CT-scan

protocol with anonymized data, adhering to ethical guidelines approved by the hospital's ethics committee. These details enhance the study's reproducibility and the generalizability of its findings.

2.3 Pre-processing (cropping, resizing, segmentation, and edge detection)

The cropping process aims to remove unnecessary noise outside the target object by trimming each edge of the object [21]. This reduction results in a focused area of interest, so any irrelevant areas outside the object's ROI are eliminated [22]. During cropping, the original data is used as input, and then this input data is cropped by manually selecting each side of the area, displaying the cropped result. Image resizing or scaling, which changes the image's size, can produce an image larger or smaller than the original [23]. In this study, the resizing process does not use a specific method. The resizing process here involves comparing the segmented image size with the target image size. Segmentation at this stage is a process aimed at isolating objects within the image or dividing the image into several regions [24]. In this study, segmentation is performed by removing the background in CT-scan images to focus specifically on the spinal image. The purpose of segmentation here is to separate the object from the background in the spinal image. Edge detection at this stage uses the Canny operator, known for optimal edge detection. This algorithm provides a low error rate, localizes edge points, and produces a single-pixel edge [25]. The purpose of edge detection is to highlight image details and improve details blurred by errors or effects from the image acquisition process.

2.4 Processing, image enhancement, and sharpening

Spinal fracture detection is a crucial process in diagnosing spinal injuries. This process typically involves several steps that employ various techniques and medical approaches to ensure an accurate diagnosis. In this study, detecting fractures in the spine involves several stages: preprocessing steps like cropping, resizing, segmentation, and edge detection. This is followed by an initial enhancement process using the LCS algorithm to identify the affected bone area and calculate its extent. Next, the development of the LCS and ROI algorithms culminates in a new algorithm called RCS, which assists in determining whether there is a fracture, thereby aiding in decision-making. Image enhancement in this study focuses on improving image quality [26]. The main purpose of image processing is to enhance the quality of an image so that it can be viewed more clearly and the information contained within it can be accurately extracted. Images that are too bright or too dark can obscure the information they contain. To improve image quality, a method is needed that can present the image effectively; contrast stretching is one such method with strong capabilities in quality improvement, able to enhance image clarity. The sharpening process in this study is a process used to sharpen image quality, namely a process that aims to clarify the edges of objects in the image [27].

2.5 LCS with ROI before development

The LCS process in this study is a process used to increase image contrast by expanding the range of pixel intensity. The pseudocode created to run the LCS and ROI programs before development can be seen in pseudocode 1.

Pseudocode 1: LCS and ROI Before Development

Input: Img
Ouput: resizedImg;
Initialization: img, normal, anomaly, luas_citra, min_contrast, max_contrast;
min_contrast = 0.1; max_contrast = 0.9;
stretched_image = imadjust(axes_image9, [min_contrast, max_contrast], []);
intensity_limit = 150;
problematic_bone = stretched_image > intensity_limit;
problematic_bone_image = cat(3, stretched_image, zeros(size(stretched_image)),
zeros(size(stretched_image)));
problematic_bone_image(repmat(problematic_bone, [1, 1, 3])) = 1;
normal_bone_image = cat(3, zeros(size(stretched_image)), stretched_image,
zeros(size(stretched_image)));
normal_bone_image(repmat(~problematic_bone, [1, 1, 3])) = 1;
result_image = normal_bone_image + problem_bone_image;
h = imrect(gca,[n/2 m/2 0.2*n 0.2*m]);
wait(h); mask = createMask(h); image_area = sum(mask(:));
points = detectSURFFeatures(rgb2gray(h_RGB));
numPoints = min(50, points.Count);
strongestPoints = points.selectStrongest(numPoints);
h_RGB_marked = insertMarker(h_RGB, strongestPoints.Location, 'color', 'red', 'size', 5);
Show normal image, anomaly, image_area

The mathematical representation of ROI and contrast functions has been updated to reflect the spatial dependencies in imaging data. Specifically, the contrast function is now defined as f(i (x, y)), where i(x, y) represents pixel intensity at spatial coordinates x and y [28]. This correction ensures consistency with imaging principles and aligns the theoretical framework with standard practices in digital image processing. The updated equations have been detailed in the methodology section to eliminate ambiguity.

The formula for LCS (linear contras stretching) can be seen from the following equation (1) [29]:

$$g(x, y) = \frac{f(x,y) - f_{min}}{f_{max} - f_{min}} * (L - 1) \quad (1)$$

The formula applies several variables, including: g(x, y) is the pixel value of the transformation result, f(x, y) is the original pixel value, f_{min} is the minimum value of a pixel in an image, f_{max} is the maximum pixel value in the image, and L is the desired scale range with a value range of 0–255 for eight bit images. While the ROI formula (*region of interest*) can be seen in equation (2) [30].

$$ROI = \frac{(x - x1)}{(x2 - x1)} * \frac{(y - y1)}{(y2 - y1)} \quad (2)$$

2.6 LCS with ROI after development

The combination of LSC and regional of interest formulas produces a new algorithm, namely RCS, which combines ROI and LCS to reflect the focus on increasing contrast in certain areas, as can be seen in equation (3).

$$g(x, y) = \left\{ \frac{f(x,y) - f_{min,}ROI}{f_{max,}ROI - f_{min,}ROI} \right\} * (L - 1) \quad (3)$$

g(x, y) is the normalized pixel intensity at a coordinate (x, y) in a resulting image [31]. Normalization aims to change the range of pixel intensity to a standard range, usually from 0 to 1 or from 0 to 255 depending on the needs.

f_{min}, ROI is the minimum pixel intensity value of a pixel in an ROI in an image. In the context of image processing, f_{min} is often used to determine the starting point of a normalization or contrast adjustment process. The f_{min} value indicates the intensity of the darkest pixel in an image, while the ROI is usually chosen based on the needs or objectives of the analysis, such as measuring a particular parameter, extracting a particular feature, or applying image processing to a particular region. f_{max}, ROI is the scope of image processing that refers to the maximum intensity value or maximum pixel intensity in an image. This is the largest pixel intensity value in the image, while ROI here explains the part that will be analyzed or processed further.

The value of L in this equation is in the context of (L – 1); L is the total number of desired intensity levels after the contrast stretching process, and (L – 1) is the maximum intensity value that can be observed under conditions. The image after processing. The higher the value of L, the greater the range of pixel intensities seen in the image. Where the formula will develop the LCS algorithm only in the marked ROI or image area, while pixels outside the ROI will retain their original values. The goal is to increase the contrast in the interesting part (ROI) without affecting other areas in the image. The first step is to provide a derivative of the existing LCS and ROI formulas with the following steps: The formula for LCS can be seen in equation (4).

$$f(x) = \frac{(x - a)}{(b - a)} \tag{4}$$

The ROI formula can be seen in equation (5) which includes the coordinates (x, y) as follows:

$$ROI = \frac{(x - x1)}{(x2 - x1)} * \frac{(y - y1)}{(y2 - y1)} \tag{5}$$

Normalization of the x-coordinate involves shifting point x so that x1 become zero. Here $x_2 - x_1$ represents the length of the ROI along the x and $\frac{x - x1}{x2 - x1}$ scales the x-coordinate to a range from 0 to 1 relative to the length of the ROI. Similarly, normalization of the y-coordinate involves shifting point y so that $y - y_1$ becomes zero. Here $y_2 - y_1$ represents the height of the ROI along the y-axis, and y and $\frac{y - y1}{y2 - y1}$ scales the y-coordinate to a range from 0 to 1 relative to the height of the ROI. The next step is to combine the two formulas, namely the LCS (linear contrast stretching) formula and the ROI (region of interest) formula, by multiplying the LCS and ROI equations. This combination represents a novelty in the research for identifying spinal fractures. The process applied in LCS and ROI is presented in equation 6.

$$g(x, y) = f(x) * ROI \tag{6}$$

So that the combination of the two formulas, namely the LCS formula and the ROI formula in equation (7).

$$g(x,y) = \frac{(x-a)}{(b-a)} * \frac{(x-x1)}{(x2-x1)} * \frac{(y-y1)}{(y2-y1)} \tag{7}$$

The proposed RCS algorithm extends traditional LCS and ROI methods by focusing on optimizing contrast enhancement within specific regions of interest. Unlike standard approaches that apply uniform adjustments, RCS selectively amplifies pixel intensity differences within a marked ROI while maintaining computational efficiency. This enhancement enables more accurate identification of subtle fracture patterns and reduces processing time. The novel combination of LCS and ROI within the RCS framework represents a significant advancement in image processing for medical diagnostics. The pseudocode created to run the LCS and ROI programs after development can be seen in pseudocode 2.

Pseudocode 2: LCS and ROI After Development

```
Input: rgbImg
Ouput: roiProcessed;
Initialization: rgbimg, roiProcessed, edges, f_min, f_max;
   grayImage = rgb2gray(rgbImage); h = imrect(handles.axes15);
   position = wait(h); roiX = round(position(1));
   roiY = round(position(2)); roiWidth = round(position(3));
   roiHeight = round(position(4));
   roi = grayImage(roiY:roiY+roiHeight-1, roiX:roiX+roiWidth-1);
   f_min = double(min(roi(:))); f_max = double(max(roi(:)));
   grayImage = double(grayImage); L = 256;
   roiProcessed = ((roi – f_min) / (f_max – f_min)) * (L – 1);
   roiProcessed = uint8(roiProcessed); edges = edge(roiProcessed, 'Canny');
   incompleteLines = imcomplement(edges); coloredImage = rgbImage;
   for i = 1:roiHeight
      for j = 1:roiWidth
         if incompleteLines(i, j) == 0
            coloredImage(roiY + i – 1, roiX + j – 1, 1) = 255;
            coloredImage(roiY + i – 1, roiX + j – 1, 2) = 0
            coloredImage(roiY + i – 1, roiX + j – 1, 3) = 0;
         end
      end
   end
      detectedArea = sum(edges(:));
      if detectedArea > 0
         status = 'Not Normal';
      else
         status = 'Normal';
      end
```

3 RESULTS

3.1 Input of CT-scan spine test image

This study was conducted in several stages. The first step is data collection. The first step in this study was to collect CT-scan images of the spine, where the images

used were 83 test images with categories of normal bone images and problematic bone images (fractures). As a sample image in this article, we display eight input images from the radiology Center of RSUP M. Djamil Padang as seen in Table 1.

Table 1. Input image

Patient	Image	Patient	Image	Patient	Image	Patient	Image
1		3		5		7	
2		4	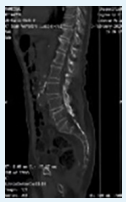	6	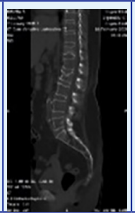	8	

3.2 Preprocessing result

Table 2 presents the results of the CT-scan spinal image preprocessing stage from the eight patients studied. This preprocessing stage includes several key steps: cropping, resizing, segmentation, and edge detection. Each step aims to improve the image quality to facilitate the process of identifying spinal fractures. By applying LCS and ROI methods, the resulting images can better highlight the spinal structure and simplify visual analysis. This approach is expected to yield more accurate fracture detection results and help radiologists accelerate the diagnostic process.

Table 2. Preprocessing result

Patient	Input Image	Cropping	Resizing	Segmentation	Edge Detection
1					
2		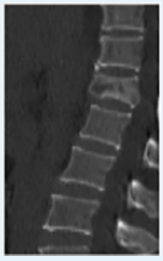	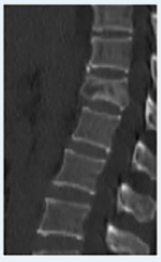		

(Continued)

Table 2. Preprocessing result *(Continued)*

Patient	Input Image	Cropping	Resizing	Segmentation	Edge Detection
3					
4	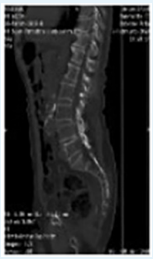				
5		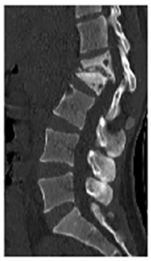			
6					
7			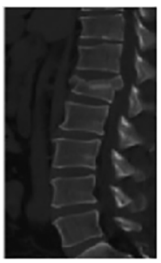		
8		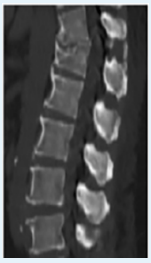	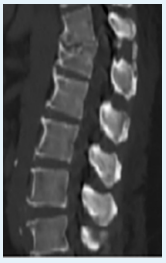		

3.3 Processing result

Table 3 shows the stages of CT-scan image processing that involve the LCS and ROI methods applied for spinal fracture detection. This process includes several key steps: edge detection, image sharpening, and the application of LCS and ROI before and after enhancement. Additionally, the final fracture detection result in the spinal area covers the initial area and post-fracture detection area in square millimeters (mm^2). Through these processing stages, LCS and ROI methods are expected to clarify bone structure and simplify the spinal fracture identification process, providing more accurate and efficient support for clinical diagnoses.

Table 3. Processing result

Patient	Edge Detection	Sharpening	LCS Before Development	LCS + ROI: After Development	Fracture (Crack) Bone Detection Results			
					Image Result	Initial Area	Image Result	New Area
1			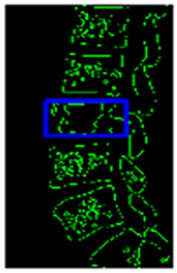			4465 mm^2		691 mm^2
2			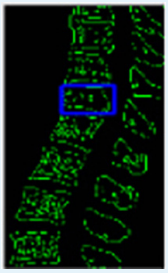		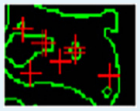	3036 mm^2		664 mm^2
3						1378 mm^2		402 mm^2
4			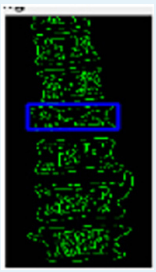		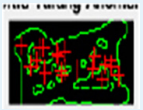	5130 mm^2		810 mm^2

(Continued)

Table 3. Processing result *(Continued)*

Patient	Edge Detection	Sharpening	LCS Before Development	LCS + ROI: After Development	Fracture (Crack) Bone Detection Results			
					Image Result	Initial Area	Image Result	New Area
5			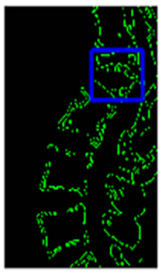	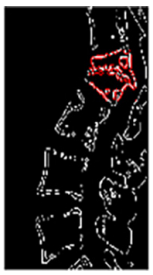	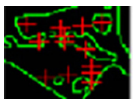	4464 mm^2		833 mm^2
6					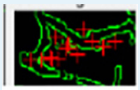	4788 mm^2		700 mm^2
7						1674 mm^2		464 mm^2
8			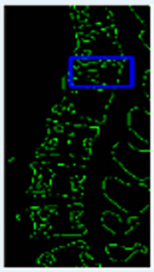			4160 mm^2		521 mm^2

To substantiate claims regarding improved image quality, the study now employs specific evaluation metrics, including pixel intensity distribution, contrast-to-noise ratio (CNR), and detection accuracy. These metrics are used to quantify the impact of LCS and ROI methods on image quality enhancement. Comparative results against baseline approaches, presented in the results section, demonstrate the superiority of the proposed method in clarifying spinal structures and enabling accurate fracture detection. In addition to quantitative findings, qualitative results are presented through annotated CT-scan images illustrating detected fractures. These visualizations highlight the specific regions identified by the RCS algorithm, providing clear evidence of its capability to focus on fracture-prone areas. By complementing numerical accuracy metrics, these annotated images enhance the interpretability and practical relevance of the study.

4 DISCUSSION

4.1 Input image discussion

Development of LCS and ROI methods for detecting spinal fractures "Based on CT-scan Images." Each image displays a sagittal view of the spine, which is crucial for identifying bone fractures with greater clarity. This table is systematically organized to facilitate visual comparisons between different cases. The use of CT-scan imaging is essential in detecting spinal fractures due to its high resolution, which enables detailed visualization of bone structures. However, conventional imaging techniques often do not clearly highlight fracture areas. Therefore, image processing methods like LCS and ROI extraction are needed. LCS enhances the contrast in critical areas, while ROI allows for focus on spine sections that are prone to fractures, minimizing interference from surrounding structures. Through the application of LCS and ROI, this method aims to provide more accurate fracture detection, assisting radiologists in making fast and precise diagnoses.

4.2 Preprocessing discussion

Based on the preprocessing results shown in Table 2, each step contributes significantly to the image quality for spinal fracture detection. The cropping stage allows focus on the spine area, removing irrelevant parts to clarify the area to be analyzed (i.e., the spine), making fractures easier to detect. The resizing stage standardizes image dimensions for consistent comparisons across patients. With uniform sizes, analysis becomes more efficient as each image has the same proportions. During the segmentation stage, the applied method can differentiate bone areas from surrounding tissue, providing clear boundaries for the spinal structure that may be fractured. Lastly, edge detection highlights the spinal contours by displaying bone boundaries, which is critical for identifying fracture-prone areas with greater precision. The edge detection results provide clear boundary visualization, enabling a deeper analysis of potential fractures. Overall, this series of preprocessing steps demonstrates the effectiveness of the LCS and ROI methods in enhancing CT-scan image quality, which is essential for supporting accurate spinal fracture detection. These results indicate the potential for clinical application, helping radiologists diagnose spinal fractures more quickly and accurately.

4.3 Processing discussion

The processing results shown in Table 3 show the effectiveness of the LCS and ROI methods in detecting fracture areas in the spine. The first step in this process is edge detection which functions to highlight the contour of the spine so that areas prone to fracture can be identified more clearly. The edge detection image, which is a clearer image of the spine, is then subjected to the second process, namely image sharpening. The image sharpening stage increases the sharpness of the details of the bone structure, which makes it easier to identify fracture patterns more accurately. This sharpened image is very good as data to be processed in the third process, namely the application of the LCS and ROI methods before and after development. The application of LCS before and after development shows significant changes in

image contrast. Before development, LCS helps highlight important areas, but after development, LCS, together with ROI, is able to focus on more specific fracture areas, so that the analysis becomes more effective. The applied ROI limits the analysis to certain areas, reduces interference from other areas in the image, and increases focus on the fracture location. The detection results show the difference between the initial area and the area after fracture detection. This difference indicates the area of fracture or cracking in the patient's spine. For example, in patient 1, the initial area was 4465 mm^2, while the new area after fracture detection decreased to 691 mm^2, indicating a specific area of fracture that was successfully isolated. Similar results were seen in other patients, where this method was able to clarify and distinguish areas of damage.

Overall, these processing stages show that the LCS and ROI methods are very effective for detecting spinal fractures. The implementation of LCS and ROI in this analysis has succeeded in increasing the accuracy and efficiency of detection, as well as providing clearer and more focused visualization of the fracture area. One of patient 1 found that the area of the image detected using the initial algorithm had an area of 4465, which was larger than the image detected using RCS. The image detected with RCS had an area of 691, where the process was carried out on images that only experienced a reduction in the spine. The application used by implementing RCS was able to read CT Scan images that experienced spinal fractures that were detected. The results showed that of the 83 input images studied, they were divided into two types, namely 43 spine images with fracture conditions and 40 spine images with normal conditions. input dataset image. By using the LCS and ROI methods that have been developed, 79 images out of 83 images can be correctly detected. To calculate accuracy, we use the formulas TP (true positive), TN (true negative), FP (false positive), and FN (false negative). Before we calculate the accuracy value, we will present the results of spinal fractures detection in CT-scan images using the TP-TN-FP-FN matrix. Below Table 4 shows the TP-TN-FP-FN matrix.

Table 4. Accuracy calculation using TP-TN-FP-FN matrix

	Predictive Positive	Predictive Negative
Actual Positive	41	2
Actual Negative	2	38

To calculate the accuracy of this study we use is formula 8 below:

$$Accuracy = \frac{TP + TN}{TP + TN + FP + FN} \tag{8}$$

$$Accuracy = \frac{26 + 28}{26 + 28 + 2 + 4} = \frac{79}{83} = 0{,}95$$

So, the percentage of accuracy in this study is 0.95 × 100% = 95%.

The detection accuracy of 95% achieved by the RCS algorithm surpasses results reported in prior studies. For instance, Jeong et al. demonstrated a 92% detection accuracy using dual-energy CT-scan technology, and Ruikar et al. reported 85% accuracy with automated segmentation. The significant improvement in accuracy underscores the effectiveness of the RCS algorithm in delivering more precise diagnostic outcomes compared to alternative methods. The diagnostic workflow of the proposed method has been clarified to highlight its practical utility. The tool

is designed as a clinician support system, requiring expert intervention for final decision-making. The system facilitates faster and more accurate preliminary diagnostics, reducing clinician workload while maintaining high diagnostic reliability. This clarification emphasizes the value of the tool in clinical environments, bridging automation with human expertise.

5 CONCLUSION

This study successfully developed the LCS and ROI methods to detect spinal fractures based on CT-scan images. Through the application of LCS, image contrast was successfully increased, allowing the bone structure to be seen more clearly. The combination with ROI allows the analysis to focus on areas suspected of having fractures so that interference from other areas in the image can be minimized. The results of the study showed that of the 80 input images studied which were divided into two types, namely 43 spinal images with fracture conditions and 40 spinal images with normal conditions, using the LCS and ROI methods that have been developed can accurately detect 41 fracture images and 38 normal images, so that it can be seen that the accuracy of this study is 79 images detected accurately from 83 images with a percentage of 95%. This method is considered effective in supporting faster and more accurate clinical diagnosis. The implementation of this method in a clinical environment can provide great benefits for the medical diagnosis process, especially in helping radiologists identify fractures more efficiently and precisely. While the RCS algorithm demonstrates promising results, its application to diverse datasets with varying CT-scan settings warrants further investigation. Additionally, the computational requirements for real-time deployment could limit its scalability in resource-constrained environments. Future research will focus on integrating deep learning techniques with the RCS framework to improve adaptability and exploring broader clinical applications in fracture diagnostics.

6 REFERENCES

[1] A. H. Trivedi *et al.*, "Robotic assisted pedicle screw placement for traumatic thoracolumbar spine fractures using the Mazor X Robot Amol," *J. Orthop. Reports*, p. 100495, 2024. https://doi.org/10.1016/j.jorep.2024.100495

[2] A. Baashar, H. Alsalman, M. Alsalman, H. Al Rehaily, and A. Alzahrani, "Spontaneous stress fracture of scapular spine associated with rotator cuff tendinopathy: A rare complication in an elderly patient," *Radiol. Case Reports*, vol. 19, no. 11, pp. 5419–5423, 2024. https://doi.org/10.1016/j.radcr.2024.07.189

[3] H. Zhao, L. Ni, G. Liu, P. Ye, and H. Duan, "Point-of-care ultrasound detection of anterior inferior iliac spine avulsion fracture in an adolescent: A case report," *Heliyon*, vol. 10, no. 15, p. e35602, 2024. https://doi.org/10.1016/j.heliyon.2024.e35602

[4] D. Murtada *et al.*, "Traumatic spine fractures and concomitant venous thromboembolism: A systematic review," *World Neurosurg. X*, vol. 24, p. 100404, 2024. https://doi.org/10.1016/j.wnsx.2024.100404

[5] M. Matthew J. Folkman, BS, Neeraj M. Patel, MD, MPH, MBS, Alexandra C. Stevens, BS, Aristides I. Cruz, Jr., MD, R. Jay Lee, MD, Indranil Kushare, MD, Theodore J. Ganley, MD, Tibial Spine Research Group, Henry Ellis, MD, Peter Fabricant, MD, Daniel Green, MD, "To manipulate or not? Management of pediatric knee arthrofibrosis following operative fixation of tibial spine fractures," *Build. Environ.*, p. 107386, 2020. https://doi.org/10.1016/j.heliyon.2024.e25108

[6] S. J. Alsufyani, M. Almurayshid, S. Ahmed Almalki, N. Mlihan Alresheedi, and T. I. Al-Naggar, "Investigating radiation shielding parameters for X-ray attenuation at various energies in locally produced ceramic materials used in Saudi Arabia," *Results Phys.*, vol. 66, p. 108006, 2024. https://doi.org/10.1016/j.rinp.2024.108006

[7] D. Iuso, P. Paramonov, J. De Beenhouwer, and J. Sijbers, "PACS: Projection-driven with Adaptive CADs X-ray Scatter compensation for additive manufacturing inspection," *Precis. Eng.*, vol. 90, pp. 108–121, 2024. https://doi.org/10.1016/j.precisioneng.2024.08.006

[8] A. E. Golbus *et al.*, "Reduced dose helical CT scout imaging on next generation wide volume CT system decreases scan length and overall radiation exposure," *Eur. J. Radiol. Open*, vol. 13, p. 100578, 2024. https://doi.org/10.1016/j.ejro.2024.100578

[9] L. C. A. Van Der Broeck, C. Mitea, D. Loeffen, M. Poeze, S. Qiu, and J. Geurts, "Assessing diagnostic accuracy: 18 F-FDG PET-CT scans in low-grade infection detection among post-traumatic long bone non-unions; a literature review and clinical data," *Injury*, vol. 55, no. S6, p. 111712, 2024. https://doi.org/10.1016/j.injury.2024.111712

[10] M. R. Willett, S. L. Codd, J. D. Seymour, and C. M. Kirkland, "Relaxation-weighted MRI analysis of biofilm EPS: Differentiating biopolymers, cells, and water," *Biofilm*, vol. 8, p. 100235, 2022. https://doi.org/10.1016/j.bioflm.2024.100235

[11] Y. Habeeb *et al.*, "High-fidelity anatomical phantoms for MRI practical training," *Phys. Medica*, vol. 127, p. 104832, 2024. https://doi.org/10.1016/j.ejmp.2024.104832

[12] T. Kim, J. Lee, and S. Kang, "Extracting common and variable code using the LCS algorithm for migration to SPLE," in *Proc. – Int. Comput. Softw. Appl. Conf.*, Torino, Italy, 2023, pp. 1004–1005. https://doi.org/10.1109/COMPSAC57700.2023.00148

[13] H. Li and P. Huang, "QR code data hiding algorithm based on cell splitting fusion with contrast stretching," in *Proc. – 2023 Int. Conf. Image Process. Comput. Vision, IPCV 2023*, 2023, pp. 127–133. https://doi.org/10.1109/IPCV57033.2023.00031

[14] H. Hendri *et al.*, "A hybrid data mining for predicting scholarship recipient students by combining K-means and C4.5 methods," *Indones. J. Electr. Eng. Comput. Sci.*, vol. 33, no. 3, pp. 1726–1735, 2024. https://doi.org/10.11591/ijeecs.v33.i3.pp1726-1735

[15] H. Hendri *et al.*, "A novel algorithm for monitoring field data collection officers of Indonesia's central statistics agency (BPS) using web-based digital technology," *Int. J. Adv. Sci. Eng. Inf. Technol.*, vol. 13, no. 3, pp. 1154–1162, 2023. https://doi.org/10.18517/ijaseit.13.3.18302

[16] I. Joshi *et al.*, "Explainable fingerprint ROI segmentation using Monte Carlo dropout," in *Proc. – 2021 IEEE Winter Conf. Appl. Comput. Vis. Work. WACVW,* 2021, pp. 60–69. https://doi.org/10.1109/WACVW52041.2021.00011

[17] Y. Ma *et al.*, "Variable rate ROI image compression optimized for visual quality," in *IEEE Comput. Soc. Conf. Comput. Vis. Pattern Recognit. Work.*, 2021, pp. 1936–1940. https://doi.org/10.1109/CVPRW53098.2021.00221

[18] W. Sun, Z. Chen, and F. Wu, "Visual scanpath prediction using IOR-ROI recurrent mixture density network," *IEEE Trans. Pattern Anal. Mach. Intell.*, vol. 43, no. 6, pp. 2101–2118, 2021. https://doi.org/10.1109/TPAMI.2019.2956930

[19] D. D. Ruikar, K. C. Santosh, and R. S. Hegadi, "Automated fractured bone segmentation and labeling from CT images," *J. Med. Syst.*, vol. 43, 2019. https://doi.org/10.1007/s10916-019-1176-x

[20] S.-Y. Jeong, S.-J. Jeon, M. Seol, T.-H. Ahn, and S. K. Juhng, "Diagnostic performance of dual-energy computed tomography for detection of acute spinal fractures," *Skeletal Radiol.*, vol. 49, pp. 1589–1595, 2020. https://doi.org/10.1007/s00256-020-03450-8

[21] A. Birhane, V. U. Prabhu, and J. Whaley, "Auditing saliency cropping algorithms," in *Proc. – 2022 IEEE/CVF Winter Conf. Appl. Comput. Vision, WACV,* 2022, pp. 1515–1523. https://doi.org/10.1109/WACV51458.2022.00158

[22] K. Apostolidis and V. Mezaris, "A web service for video smart-cropping," in *Proc. – 23rd IEEE Int. Symp. Multimedia,* 2021, pp. 25–26. https://doi.org/10.1109/ISM52913.2021.00011

[23] H. Wang *et al.*, "Bamboo filters: Make resizing smooth," in *Proc. – Int. Conf. Data Eng.*, 2022, pp. 979–991. https://doi.org/10.1109/ICDE53745.2022.00078

[24] Y. Liang, R. Wakaki, S. Nobuhara, and K. Nishino, "Multimodal material segmentation," in *Proc. IEEE Comput. Soc. Conf. Comput. Vis. Pattern Recognit.*, vol. 2022, pp. 19768–19776, 2022. https://doi.org/10.1109/CVPR52688.2022.01918

[25] N. Anuar, Z. Abu Bakar, and N. K. Ismail, "Extraction of Malay root word that starts with letter P in Malay e-Khutbah using rule based," *International Journal of Software Engineering and Computer Systems*, vol. 9, no. 1, pp. 39–45, 2023. https://doi.org/10.15282/ijsecs.9.1.2023.4.0108

[26] N. S. Yan and R. Mohamed, "Feasibility study on using MCDM for e-voting," *International Journal of Software Engineering and Computer Systems*, vol. 8, no. 2, pp. 1–9, 2022. https://doi.org/10.15282/ijsecs.8.2.2022.1.0098

[27] E. Erni and D. Riana, "Deep neural network for click-through rate prediction," *International Journal of Software Engineering and Computer Systems*, vol. 8, no. 2, pp. 33–42, 2022. https://doi.org/10.15282/ijsecs.8.2.2022.4.0101

[28] F. Titiani and D. Riana, "Ensemble learning for the prediction of marketing campaign acceptance," *International Journal of Software Engineering and Computer Systems*, vol. 8, no. 2, pp. 67–76, 2022. https://doi.org/10.15282/ijsecs.8.2.2022.7.0104

[29] M. S. Azmi, M. M. Izham, M. H. Jalil, and M. H. Mazlan, "CT-FEA of inhomogeneous lumbar with different loadings of the spinal cage," *International Journal of Automotive and Mechanical Engineering*, vol. 20, no. 4, pp. 10894–10905, 2023. https://doi.org/10.15282/ijame.20.4.2023.07.0842

[30] N. S. M. Salleh, M. H. Mazlan, and M. A. Razali, "Comparative biomechanical evaluation of unilateral and bilateral cages in posterior lumbar interbody fusion: Endplates subsidence, pedicle screw loosening and implant stability," *International Journal of Online and Biomedical Engineering*, vol. 19, no. 18, pp. 123–138, 2023. https://doi.org/10.3991/ijoe.v19i18.43833

[31] M. S. F. Ramli, M. H. Mazlan, H. Takano, A. H. Abdullah, and M. H. Jalil, "A review of material, design, and techniques in 3D printing for medical applications," *International Journal of Online and Biomedical Engineering*, vol. 19, no. 16, pp. 38–64, 2023. https://doi.org/10.3991/ijoe.v19i16.40855

7 AUTHORS

Sri Rahmawati is a Lecturer at the Information Systems study program, Faculty of Computer Science, Universitas Putra Indonesia YPTK Padang. She did her under graduation in the Information Systems Study Program, UPI YPTK Padang and her Masters in the Computer Science, UPI YPTK Padang. She is currently pursuing Ph.D., in the Information Technology Doctoral Study Program, UPI YPTK Padang. Her expertise is in the fields of image processing, databases. and information systems. She can be contacted via email at sri_rahmawati@upiyptk.ac.id.

Iskandar Fitri is a Professor at Universitas Putra Indonesia YPTK Padang, serving as a lecturer in the information technology doctorate program within the Faculty of Computer Science. His academic journey includes completing his undergraduate education (S1) in the electronics engineering study program at Universitas Nasional, followed by Master's (S2) and Doctoral (S3) degrees in the electronics engineering study program at Universitas Indonesia. Presently, he is recognized as a professor specializing in the microwave field at UPI YPTK Padang, for offering a diverse

array of courses in the information technology study program, such as microwaves, research methodology, and artificial intelligence, for communication. He can be reached via email at if@upiyptk.ac.id.

Gunadi Widi Nurcahyo is a Lecturer at the Department of Master of Informatics Engineering (S2), Faculty of Computer Science, Universitas Putra Indonesia YPTK Padang, West Sumatra, Indonesia. He earned his Bachelor's degree from Universitas Putra Indonesia YPTK Padang in the Information Systems study program, Faculty of Computer Science. Then continued his Master's (M.Sc.) and Doctoral (Ph.D.) studies at the University of Technology Malaysia (UTM), Malaysia, specializing in Computer Science. Halifia's unique identifier, Scopus ID, is 57201027973. His research efforts span across multiple domains, with special expertise in data science, and computer science. Gunadi welcomes communication and collaboration, and can be contacted via email at gunadiwidi@yahoo.co.id.